NRC Research Press

ARTICLE

Continuous medium hypothesis-based study on the screw flight wear model and wear regularity in a screw ship unloader

Weijie Yang, Wenjun Meng, Xiaobing Dai, Zhenxiao Yin, Fenglin Yao, and Yuan Yuan

Abstract: Screw flight on a vertical screw conveyor, which is a spiral blade welded on an axial cylinder, is the core component of a screw ship unloader and can be seriously worn by the materials during long-term conveying. Damaged screw flights make the screw ship unloader unable to unload materials or even lead to an accident. Hence, we established a new screw flight wear model based on the Archard wear model and continuous medium hypothesis. Two influencing factors, speed and filling rate, were selected to study the wear law of the screw flight, and the wear law was verified experimentally. The results indicate that the experimental results were consistent with the calculation model. The wear rate of the screw flight was approximately parabola-increased with the increase in rotational speed, and the screw flight wear rate positively and linearly correlated with the filling rate.

Key words: screw ship unloader, screw flight, wear, archard wear model, continuous medium hypothesis.

Résumé : La vis sans fin du convoyeur à vis vertical, qui consiste en une lame en spirale soudée au cylindre axial, constitue le composant essentiel du déchargeur à vis et peut être sérieusement usée par les matériaux pendant le transport à long terme. Si la vis est endommagée, le déchargeur à vis est incapable de décharger les matériaux ou peut même provoquer un accident. Nous avons donc établi un nouveau modèle d'usure de la vis basé sur le modèle d'usure d'Archard et l'hypothèse du milieu continu. Deux facteurs d'influence, dont la vitesse et le taux de remplissage, ont été sélectionnés pour étudier la loi d'usure de la vis, et la loi d'usure a été vérifiée par des expériences. Les résultats indiquent que les résultats expérimentaux étaient conformes au modèle de calcul. Le taux d'usure du filet de la vis est approximativement en parabole avec l'augmentation de la vitesse de rotation et le taux d'usure du filet de la vis est positivement et linéairement corrélé avec le taux de remplissage. [Traduit par la Rédaction]

Mots-clés : déchargeur de navires à vis, vol de vis, usure, modèle d'usure d'Archard, hypothèse du milieu continu.

1. Introduction

The vertical screw conveyor is mainly used in port screw ship unloaders to load and unload coal or crops and has the characteristics of low energy consumption, high transmission efficiency, and capacity to lift more materials (Sun et al. 2018). The vertical screw conveyor is the core component of the screw ship unloader, and its performance directly affects the reliability and service life of the screw ship unloader. The failure of the vertical screw unloader mainly manifests as the wear of the screw flight. The material particles strongly collide with the screw flight, which causes the screw flight to be worn seriously. The severely worn screw flight often leads to downtime accidents, delays production, and reduces the service life of the screw ship unloader.

In recent years, many scholars have conducted research on the wear of equipment for conveying bulk materials (such as scraper conveyors and screw conveyors) and found that the wear types of equipment wear

Received 9 December 2020. Accepted 30 March 2021.

W. Yang and W. Meng. School of Mechanical Engineering, Taiyuan University of Science and Technology, Taiyuan 030024, China.

X. Dai and Z. Yin. Institute for Materials Handling, Material Flow and Logistics, Technical University of Munich, Boltzmannstraße 15, Garching 85748, Germany.

F. Yao and Y. Yuan. Key Laboratory of Intelligent Logistics Equipment in Shanxi Province, Taiyuan University of Science and Technology, Taiyuan 030024, China.

Corresponding author: Wenjun Meng (email: tyustmwj2021@163.com).

are mainly abrasive wear but also include fatigue and erosion wear (Moore 1978; Piazzetta et al. 2018).

The Archard wear model is a commonly used model for analyzing material wear (Archard 1953). The wear coefficient K, positive pressure F_n, and sliding distance S are the key factors that constitute the Archard wear model. The wear coefficient K is related to the inherent properties of the conveying bulk materials, including hardness, particle shape, and particle size. Many scholars have studied the wear coefficient K and sliding distance S of different materials based on the Archard wear model. Bialobrzeska and Kostencki (2015) studied the wear coefficient of low-alloy boron steel based on the Archard wear model and found that during the friction process between particles and low-alloy boron steel, the particles with larger hardness flake off and cause larger scratches. Chen et al. (2017) used the Archard wear model to study single-particle sliding wear, and the results indicated that an increase in particle density or radius would cause more steady-state sliding wear at the single-particle level. The Archard wear model (Forsström and Jonsén 2016; Gong et al. 2016; Wang et al. 2017) was used to study the wear of the crusher lining by exploring different particle sliding distances, and the numerical calculation showed that an increase in the particle sliding distance would increase the crusher wear.

Positive pressure F_n is a key factor in the Archard wear model. Normally, the positive pressure F_n is set as a constant in the numerical calculation of the material wear. This setting may reduce the accuracy of computing equipment wear. To reduce calculation errors, the EDEM software, which loaded the Archard wear model, calculated the force of particle collision on the surface of the equipment at different times and the positive pressure F_n of the equipment at different times by statistics to analyze the wear of the equipment. Wang et al. (2018) used the EDEM software to analyze the bulk coal transport state of a scraper conveyor and confirmed that the key reason for the failure of the scraper conveyor chutes caused by the coal was abrasive wear. This study proves that the Archard wear model can predict equipment wear well. Xia et al. (2019) also used EDEM software to study the wear of a scraper conveyor and verified the accuracy of the simulation results through experiments. Yang (2019) used the EDEM software to study the wear of the screw flight under different conditions by changing the filling rate, speed, and pitch. The results indicated that as the filling rate increased, the rotational speed increased, the pitch decreased, and the wear of the screw flight increased. The EDEM software based on the discrete element method has been used by more scholars to study the wear of equipment for conveying different bulk materials, and the accuracy of its calculation results has been verified by different experiments.

Considering the macroscopic mechanical properties of a large number of particles, the method of obtaining the positive pressure of the scattered particles includes the continuous medium hypothesis method. German engineer Janssen (1895) proposed the use of the continuum model to analyze the static stress of the silo in 1895, and this method has been widely recognized. Rahmoun et al. (2008) developed a continuous media approach for the calculation of the stresses in an ensiled granular medium, which improves on the Janssen theory, and the continuous media approach allowed us to qualitatively and quantitatively represent the stress saturation phenomenon in granular silos. Wang et al. (2015) compared the discrete element comparison with the hydrodynamic approach under the same set of rheological laws, material parameters, and numerical method, and the stresses predicted by the two approaches match well the inflow zones. Wang et al. (2019) used the continuous medium hypothesis to study the positive pressure of activated coke particles in an absorption tower and verified through experiments that the continuum model can effectively describe the mechanical properties of the activated coke particles in the absorption tower.

This study established a screw flight wear model based on the Archard wear model, which used the continuous medium hypothesis to calculate the positive pressure F_n at different positions of the bulk in the vertical screw conveyor. We then analyzed the relationship between the different influencing factors and screw flight wear. Finally, the model was experimentally verified by analyzing the rotational speed and filling rate.

2. Theory and Method

2.1. Model of the vertical screw conveyor

The overall structure of the screw ship unloader is shown in Fig. 1 (Pratap et al. 2017). Its structure mainly includes a vertical screw conveyor, feeding head, horizontal conveyor, truss, and other components (Song et al. 1995). However, the vertical screw conveyor is the core component of the screw ship unloader, and its main structure includes screw flight, shell, motors, and other parts. The process of unloading materials of the screw ship unloader is as follows: first, the screw ship unloader inserts the vertical screw conveyor into the material to be unloaded; second, the material is gathered to the feed port under the push of the feeding head; third, the vertical screw conveyor vertically lifts material; and finally, the horizontal conveyor conveys the material to the scheduled receiving place.

In the process of loading and unloading materials, the strong relative collision between the screw flight and the material causes the screw flight to be worn seriously. For screw-ship unloaders, monitoring the wear of the screw flight under their working conditions is dangerous and difficult to achieve. Moreover, the screw ship unloaders in different ports have varying working conditions for lifting and conveying different materials, which results in varying wear conditions. Therefore, it is necessary to

Fig. 1. Screw ship unloader: (*a*) model of screw ship unloader; (*b*) diagram of coal unloading using a screw ship unloader. [Colour online.]

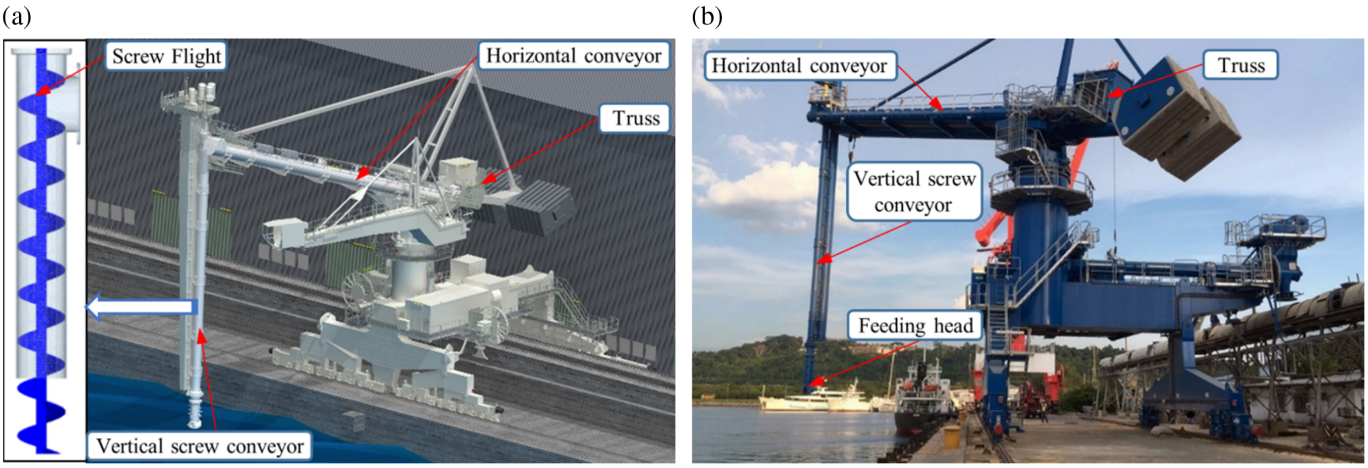

establish a wear model to predict screw flight wear under different working conditions.

2.2. Screw flight wear model

2.2.1. *The Archard wear model*

In the study of wear, Archard (1953) established the classic Archard wear model. The Archard wear model mainly expresses the relative friction between the material and the geometry. The greater the volume of the material removed by the irregular-shaped particles, the more the work done by the relative displacement of the material on the surface of the geometry. The Archard wear model is as follows:

$$Q = W \cdot F_n \cdot S \tag{1}$$

$$W = \frac{K}{\text{Hardness}} \tag{2}$$

where Q is the relative wear, K is the dimensionless constant, Hardness is the surface hardness of the material, F_n is the positive pressure at the wear location, and S is the displacement of the force.

2.2.2. *Establishment of the screw flight wear model*

The wear model of the screw flight can be established based on the Archard wear model and the continuous medium hypothesis of the coal particles in the vertical screw conveyor. The relative displacement of the particles per unit time was calculated using the single-particle method, and the positive pressure F_n was calculated using the continuous medium hypothesis.

First, the relative displacement of the particles per unit time was calculated. When the material begins to exhibit the limit of vertical upward movement, the force acting on the particle where the surface of the screw flight contacts the shell is shown in Fig. 2 under the rotation of the screw flight.

Fig. 2. Schematic of single-particle force. [Colour online.]

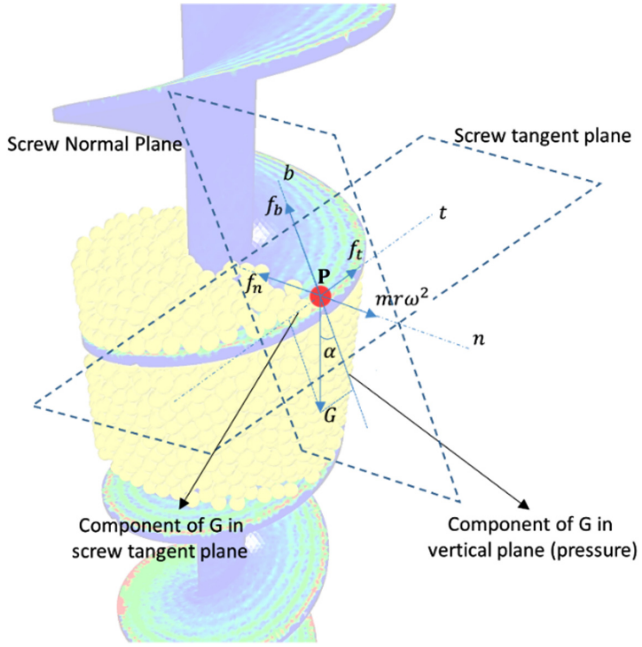

As shown in Fig. 2, the screw tangent plane (*nt*) and the screw normal plane (*nb*) along the screw plane direction were set at point P, where the particle was located. The t is the tangential direction in the screw tangent plane (*nt*), b is the normal direction in the normal plane (*nb*) of the screw, and n is the normal direction of point P relative to the screw shaft. f_n is the supporting force of the screw conveyor shell to the particle, f_b is the supporting force of the screw flight to the particle, and f_t is the resultant force of the friction generated by the particle, the screw flight surface, and the screw conveyor shell.

In this extreme case, gravity, centrifugal force, and frictional forces on the particles should be in equilibrium.

Fig. 3. Four types of material filling with the same screw parameters. [Colour online.]

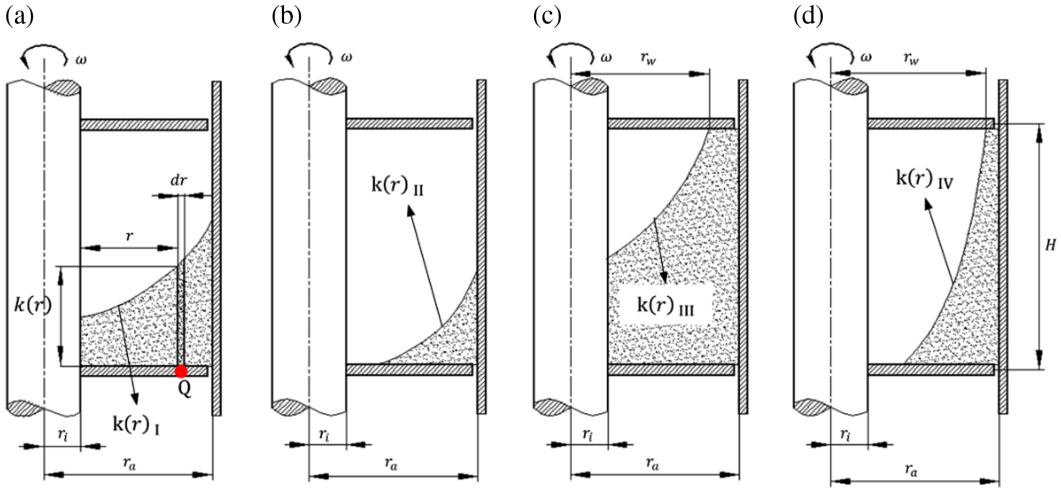

$$(3)\quad f_t = \frac{m\cdot v_k^2}{r}\cdot\mu_g\cdot(\cos\alpha-\mu_p\cdot\sin\alpha) - m\cdot g\cdot\mu_p\cdot\cos\alpha = m\cdot g\cdot\sin\alpha$$

According to the Moiré stress circle diagram of particles in bulk mechanics (Knuth et al. 2012), the maximum ratio of shear stress τ to compressive stress σ is the internal friction coefficient μ_p of the material.

$$(4)\quad \mu_p = \mathrm{tg}\beta = (\tau/\sigma)_{\max}$$

According to eqs. 3 and 4, the circumferential velocity v_k of the particle under this limit is

$$(5)\quad v_k = \sqrt{\frac{r\cdot g}{\mu_g}\mathrm{tg}(\alpha+\beta)}$$

where g is the acceleration of gravity, m is the mass of the particle, r is the screw flight radius, μ_p is the coefficient of friction between the particle and the screw flight, μ_g is the coefficient of friction between the particle and the screw conveyor shell, α is the inclination angle of the spiral surface in Fig. 2, and β is the friction angle between the particle and the spiral surface.

The speed of the screw flight at the particle is v_s. Thus, the relative speed v_{sk} between the particle phase and the screw flight is

$$(6)\quad v_{sk} = (v_s - v_k)\cdot\cos\alpha$$

The relative displacement of particle in a unit of time is

$$(7)\quad \mathrm{d}s = v_{sk}\cdot\mathrm{d}t$$

$$(8)\quad \mathrm{d}s = \left(v_s - \sqrt{\frac{r\cdot g}{\mu_g}\mathrm{tg}(\alpha+\beta)}\right)\cos\alpha\cdot\mathrm{d}t$$

Table 1. Types of $k(r)$.

Case	Range of material filling rate
$k(r)_{\mathrm{I}}$	$k(r) = k^* + \frac{\omega^2}{2g}\cdot r^2 \quad k^* > 0 \quad r_i \le r \le r_a$
$k(r)_{\mathrm{II}}$	$k(r) = \begin{cases} k^* + \frac{\omega^2}{2g}\cdot r^2 & k^* < 0 \quad r_b \le r \le r_a \\ 0 & k^* < 0 \quad r_i \le r \le r_b \end{cases}$
$k(r)_{\mathrm{III}}$	$k(r) = \begin{cases} k^* + \frac{\omega^2}{2g}\cdot r^2 & k^* > 0 \quad r_i \le r \le r_w \\ H & k^* > 0 \quad r_w \le r \le r_a \end{cases}$
$k(r)_{\mathrm{IV}}$	$k(r) = \begin{cases} k^* + \frac{\omega^2}{2g}\cdot r^2 & k^* < 0 \quad r_b \le r \le r_w \\ 0 & k^* < 0 \quad r_i \le r \le r_b \\ H & k^* < 0 \quad r_w \le r \le r_a \end{cases}$

Second, the continuous medium hypothesis was used to analyze the positive pressure F_n at different positions of the equipment. As shown in Fig. 3*a*, the resultant force on the screw flight at point Q is the resultant force of all particles in the dr width above the Q point, as follows:

$$(9)\quad F_n = M\cdot\cos\alpha + \frac{M\cdot v_k^2}{r}\cdot\mu_s\cdot\sin\alpha$$

$$(10)\quad M = \rho\cdot g\cdot k(r)\cdot\frac{\pi}{4}\cdot D_p^2$$

where M is the total mass of all particles stacked above a certain point of the screw flight, $k(r)$ is the particle stack height in Fig. 3*a*, ρ is the particle density, and μ_s is the sliding friction coefficient between the particles.

Table 2. Design parameters of the screw flight.

Case	Influencing factor
Wear coefficient, K	3.685e–4
Hardness of steel	HRC20
Radius of screw flight, r_a	100 mm
Angle between spiral section and horizontal plane, α	13.4°
Coefficient of friction between particles and the shell of screw conveyor, μ_g	0.4
The radius of spiral shaft, r_i	20 mm
Screw rotational speed, ω	100–500 rpm
Filling rate, φ	0–1
Pitch of screw flight, H	150 mm

Fig. 4. Wear rate of the screw flight under different rotational speed ω and filling rate φ. [Colour online.]

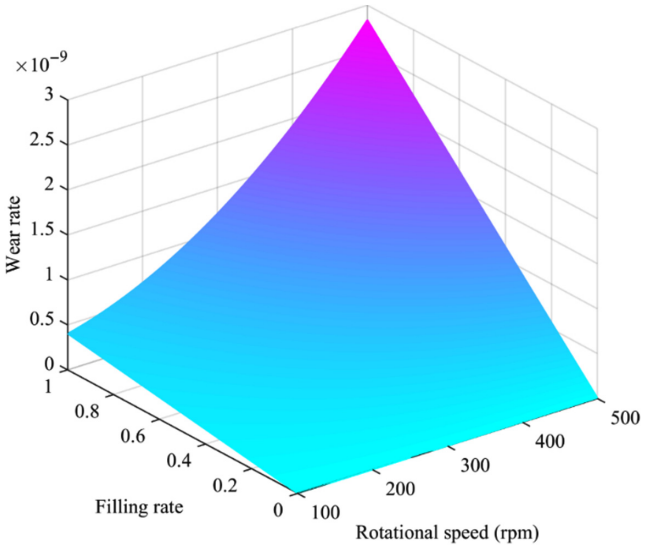

The actual screw conveying material cannot fill the entire vertical screw conveyor and moves to the side of the shell under the action of centrifugal force. The filling types of the material under the same screw parameters are shown in Figs. 3*a*–3*d*.

$k(r)$ is solved following the parabolic equation of the rotating liquid proposed by Gabler (1981) as the initial equation theory. The equation is as follows:

$$k(r) = k^* + \frac{\omega^2}{2g} \cdot r^2 \tag{11}$$

where k^* is determined by calculating the volume of the rotating body in the Guldinschen Regel law (Neuendorff 1919). The equation is as follows:

$$V = 2 \cdot \pi \cdot \int_{r_i}^{r_a} r \cdot k(r) \cdot dr \tag{12}$$

$$V = \varphi \cdot (r_a^2 - r_i^2) \cdot \pi \cdot H \tag{13}$$

$$V = 2 \cdot \pi \cdot \int_{r_i}^{r_a} r \cdot \left(k^* + \frac{\omega^2}{2g} \cdot r^2 \right) \cdot \mathrm{d}r = \varphi \cdot (r_a^2 - r_i^2) \cdot \pi \cdot H \tag{14}$$

Using eqs. 8, 9, and 10, the wear model of the screw flight can be established as

$$\mathrm{d}Q = W \cdot F_n \cdot \mathrm{d}S \tag{15}$$

$$\frac{\mathrm{d}Q}{\mathrm{d}t} = \frac{K}{\text{Hardness}} \cdot \rho \cdot g \cdot k(r) \cdot \frac{\pi}{4} \cdot D_p^2 \left(g \cdot \cos\alpha + \frac{v_k^2}{r} \cdot \mu_s \cdot \sin\alpha \right) \cdot \left(v_s - \sqrt{\frac{r \cdot g}{\mu_g} \mathrm{tg}(\alpha + \beta)} \right) \cos\alpha \tag{16}$$

The average wear rate of all points along the line from particle P to the helix axis in the n direction is

$$\frac{\mathrm{d}Q}{\mathrm{d}t_{\text{average}}} = \frac{K}{\text{Hardness}} \left(g \cdot \cos\alpha + \frac{v_k^2}{r} \cdot \mu_s \cdot \sin\alpha \right) \cdot \left(v_s - \sqrt{\frac{r \cdot g}{\mu_g} \mathrm{tg}(\alpha + \beta)} \right) \cos\alpha \cdot \rho \cdot g \cdot \frac{\int_{r_i}^{r_a} k(r)\mathrm{d}r}{(r_a - r_i)} \cdot \frac{\pi}{4} \cdot D_p^2 \tag{17}$$

According to the different material filling types in Fig. 3, $k(r)$ can be calculated using eqs. 11, 12, 13, and 14 as

Fig. 5. Experimental device of vertical screw conveyor: (*a*) experimental device; (*b*) schematic diagram of the experiment; (*c*) wear appearance of the screw flight. [Colour online.]

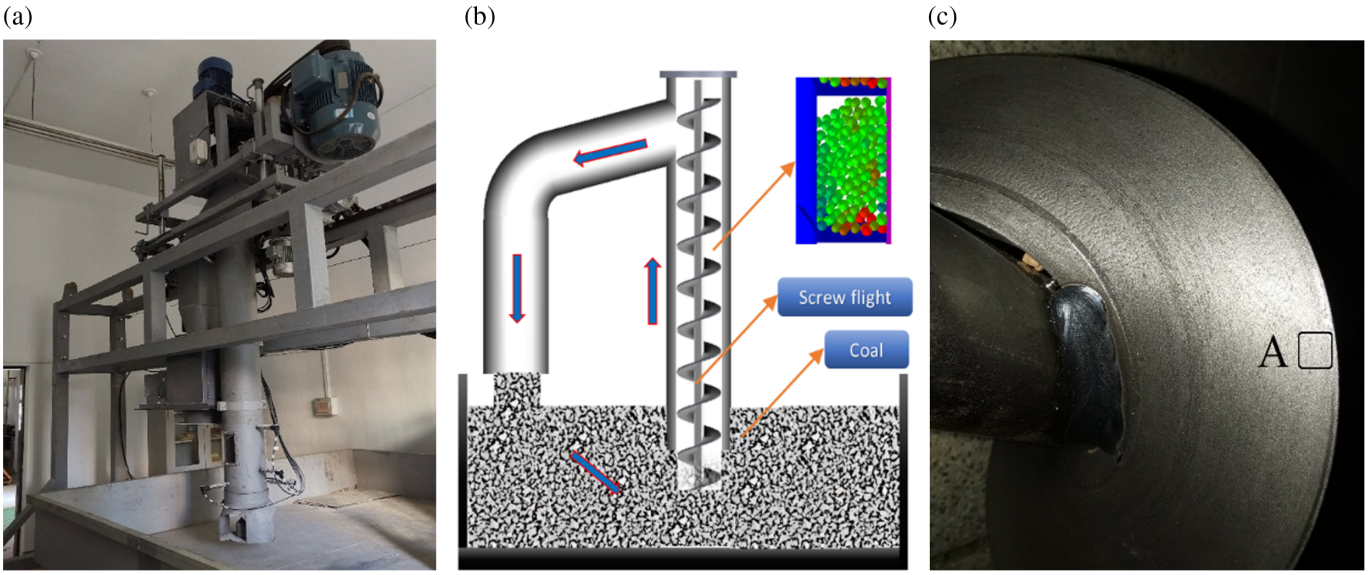

$$(18)\quad \begin{cases} k(r)_{\mathrm{I}} = \varphi \cdot H - \dfrac{\omega^2}{4 \cdot g} \cdot (r_a^2 + r_i^2) + \dfrac{\omega^2}{2 \cdot g} \cdot r^2 \\ k(r)_{\mathrm{II}} = \omega \cdot r_a \cdot \sqrt{\dfrac{H \cdot \varphi \cdot (r_a^2 - r_i^2)}{g \cdot r_a^2}} - \dfrac{\omega^2}{2 \cdot g} \cdot (r_a^2 - r^2) \\ k(r)_{\mathrm{III}} = H - \omega \cdot \sqrt{\dfrac{H}{g} \cdot \left[r_a^2 \cdot \left(1 - \varphi \cdot \dfrac{r_a^2 - r_i^2}{r_a^2} \right) - r_i^2 \right]} + \dfrac{\omega^2}{2 \cdot g} \cdot (r^2 - r_w^2) \\ k(r)_{\mathrm{IV}} = H + \dfrac{\omega^2}{2 \cdot g} \cdot \left[r^2 - \dfrac{H \cdot g}{\omega^2} - r_a^2 \cdot \left(1 - \varphi \cdot \dfrac{r_a^2 - r_i^2}{r_a^2} \right) \right] \end{cases}$$

where φ is the filling rate of the material in the screw flight, H is the pitch, ω is the speed of the screw flight, r_i is the radius of the screw shaft, and r_a is the radius of the screw flight.

The filling rate of the material in the screw flight is

$$(19)\quad \varphi = \frac{V_C}{V}$$

where V_C is the volume of material, which is expressed as

$$(20)\quad V_C = 2 \cdot \pi \cdot \int_{r_i}^{r_a} r \cdot k(r) \cdot \mathrm{d}r$$

and the V is the space volume, which is expressed as

$$(21)\quad V = \pi \cdot H \cdot (r_a^2 - r_i^2)$$

Among them, as shown in Table 1, the type of $k(r)$ can be determined by the parameters k^* and the range of variables r in the vertical screw conveyor.

2.3. Theoretical analysis and calculation of the screw flight wear model

Two key variables, the screw flight speed ω and material filling rate φ, were used to study the influence of the screw flight wear model on the wear rate. The Chinese standard LX-200 screw ship unloader was selected for the wear research. The material used for the screw flight was a Q235A plain carbon structural steel. The parameters of the screw flight are listed in Table 2.

Coal was selected to study the wear of the screw flight. Owing to the small change in the surface temperature of the screw flight during coal transportation, the Hardness of coal was regarded as a constant. The diameter of the coal particles was 16 mm. The density ρ was 1500 kg/m^3. The friction angle β between the particles and the screw flight was 21.77°. The sliding friction coefficient between the particles μ_s was 0.6.

Figure 4 shows the variation trend of the wear rate of the screw flight at different rotational speeds and filling

Fig. 6. Three-dimensional profile images of the worn screw flight surface: (*a*) 120 rpm rotational speed; (*b*) 200 rpm rotational speed; (*c*) 280 rpm rotational speed; (*d*) 360 rpm rotational speed. [Colour online.]

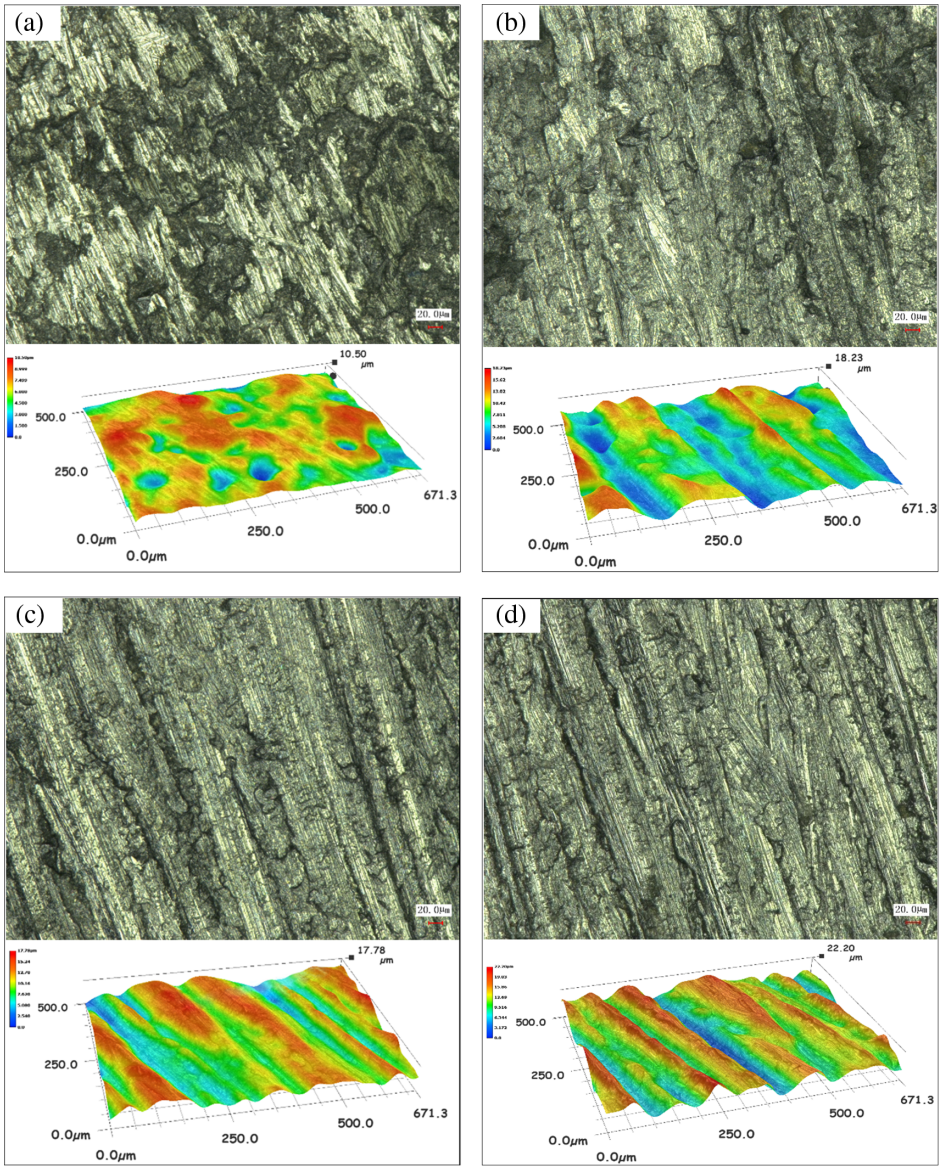

rates calculated by the MATLAB software. With an increase in the rotational speed and filling rate, the wear rate of the screw flight increases. When the filling rate was 1 and the rotational speed was 500 rpm, the wear rate of the screw flight was the highest at 2.837e–9. When the material filling rate is constant, the wear rate shows a parabolic increase with the increase in rotational speed and the growth rate from slow to fast. The increase in the relative rotational speed of coal and screw flight accelerates the surface wear of the screw flight. With an increase in the filling rate, which increases the positive pressure F_n acting on the surface of the screw flight, the wear rate of the screw flight increases linearly in the theoretical model. Therefore, the model can be used to predict the wear of the screw flight under different conditions.

3. Experimental verification

As shown in Fig. 5*a*, the vertical screw conveyor device used in this study comprised a feeding system, vertical screw conveying system, discharge system, x–y–z motion system, and workbench. As shown in Fig. 5*b*, the coal in the chute was transported vertically upward through the vertical screw conveyor, and then the coal fell into the chute from the discharge pipe. In this test, eight sets of screw flights with the same specifications were selected for replacement under different test conditions, including different speeds and filling rates. Each screw flight was operated for 24 h to observe its wear. Figure 5*c* shows the wear appearance of the screw flight at a filling rate of 0.8, and a speed of 200 rpm. The outermost part of the screw flight was severely worn; therefore, area A in the screw flight was selected as the

Fig. 7. Three-dimensional profile images of the worn screw flight surface: (*a*) 0.2 filling rate; (*b*) 0.4 filling rate; (*c*) 0.6 filling rate; (*d*) 0.8 filling rate. [Colour online.]

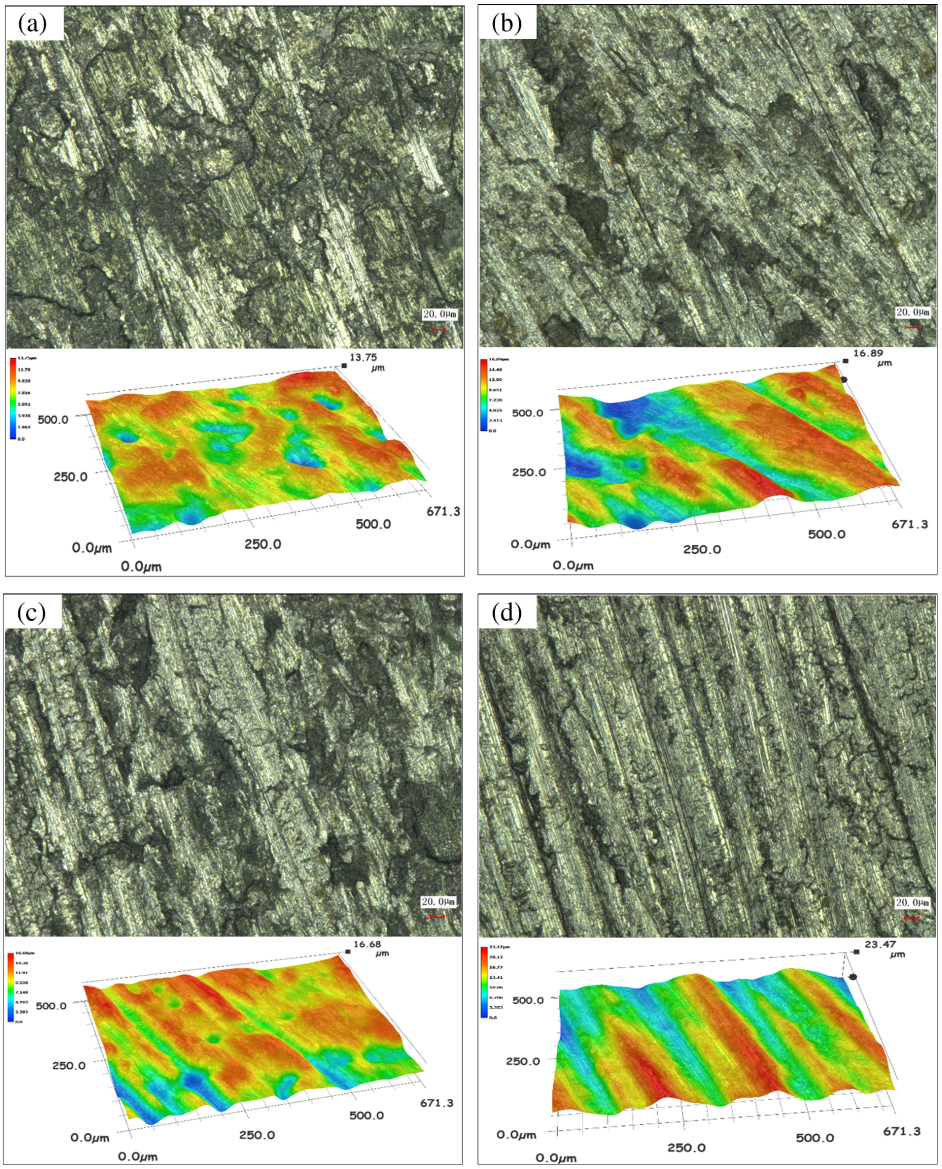

research object. A Keyence VHX-2000 super-depth-of-field microscope with a magnification range of 0.1–5000 was used to observe the surface morphology of the worn screw flight.

As shown in Fig. 6*a*, at a rotational speed of 120 rpm, there are a few pits and small convex peaks on the surface of the screw flight caused by abrasive wear and a small amount of impact wear. The depth of the pits was concentrated at approximately 7.8 μm. At a rotational speed of 200 rpm (Fig. 6*b*), numerous pits and small convex peaks appeared on the worn surface. When the speed increases to 280 rpm (Fig. 6*c*) and 360 rpm (Fig. 6*d*), regular furrows appear on the wear surface caused by the long-term abrasive wear of coal, which has a relative speed with the screw flight. When the rotational speed was 360 rpm, the screw flight wear was the most serious, and the wear scar was full of deep and dense furrows, which is a typical abrasive wear feature. The greater the average velocity of the coal particles, the greater the relative velocity between the coal and screw flight, and the more serious the screw flight wear.

As the filling rate increased, the width and depth of the screw flight wear increased. Figures 7*a*–7*b* show that for the filling rates of 0.2 and 0.4, light wear is shown, and only a small number of pits appear on the blade surface. Figure 7*c* shows that there are a few irregular furrows on the spiral surface for a filling rate of 0.6. When the material filling rate is 0.8, as shown in Fig. 7*d*, the spiral surface has a relatively regular wear morphology of

Fig. 8. Comparison of the wear rate fitting curves of theoretical model and experiment: (*a*) wear rate for different rotational speeds; (*b*) wear rate for different filling rates. [Colour online.]

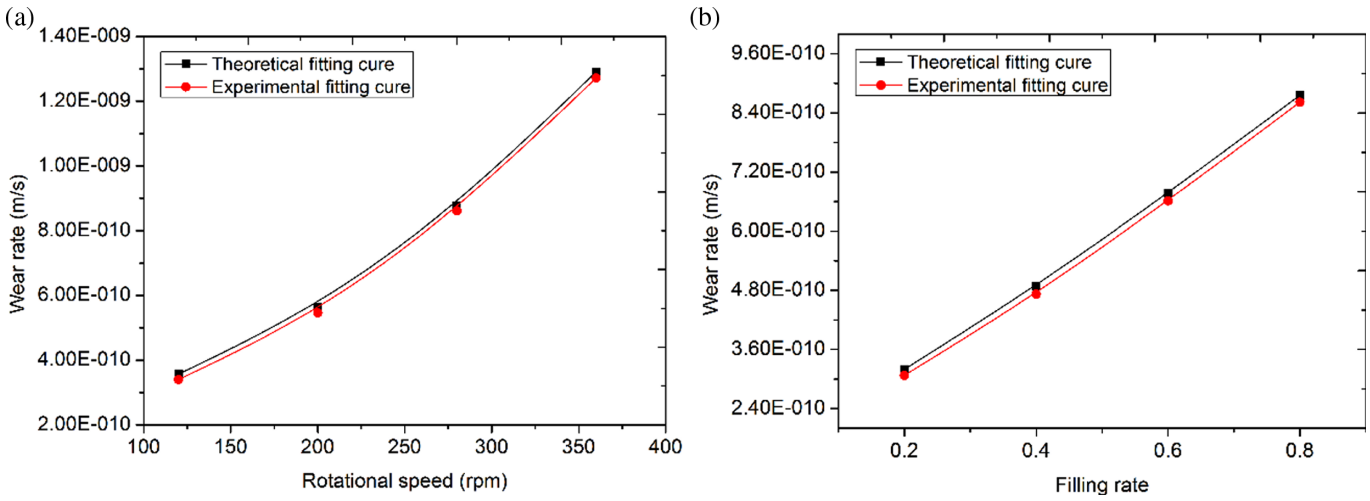

the furrow, and the maximum depth of the furrow is 13.8 μm. Figure 7 shows that with an increase in the filling rate, the positive pressure F acting on the surface of the screw flight increases, resulting in intensified wear of the screw flight.

4. Discussion

The wear trend of the screw flight was fully described by analyzing the wear condition of the screw flight in the experiment. The wear rate in the experiment, $\left(\frac{dQ}{dt}\right)_E$, which can be defined in terms of the average wear depth h_E and wear time, is

$$\left(\frac{\mathrm{d}Q}{\mathrm{d}t}\right)_E = \frac{\Delta S \cdot h_E}{t} \quad (22)$$

where ΔS is the unit wear area and t is the wear time in the experiment.

To further verify the accuracy of the model, the wear rate curve of the screw flight wear model was compared with the experimental fitting curve.

Figure 8 shows that the experimental results are consistent with the calculation model, and the trends of the wear curves are the same. Figure 8*a* shows a comparison diagram of the theoretical wear rate curve and experimental fitting wear rate curve under different rotational speeds. With the increase in rotational speed, the wear rate of screw flights increases with a parabolic trend in the theoretical model and experiment. The increase in rotational speed leads to an increase in the mass flow of the material at the same time. The increase in the relative rotational speed between coal and screw flight accelerates the surface wear of the screw flight. Figure 8*b* shows a comparison diagram of the theoretical wear rate curve and experimental fitting wear rate curve under different filling rate conditions. With an increase in the filling rate, the wear rate of the screw flight increases linearly in the theoretical model and experiment. The increase in the filling rate, which increases the positive pressure F_n acting on the surface of the screw flight, leads to an increase in the wear rate.

However, it can be observed from Fig. 8 that the theoretical wear rate is greater than the experimental wear rate under the same working conditions. This is because the number of blade wear points calculated by the theoretical model is greater than the number of experimental wear points. There are gaps between the particles in the experiment, and the blade does not contact the particles; therefore, the statistics of the total wear points of the blades are reduced. However, in the theoretical model, based on the continuous medium hypothesis, the amount of wear at all points on the blade was counted.

Hence, the screw flight wear model can be used to predict the wear of the screw flight of a vertical screw conveyor under different working conditions. It also provides a reliable calculation model for screw flight life prediction.

6. Conclusion

Based on the Archard wear model and the continuous medium hypothesis of the coal particles in the vertical screw conveyor, this study constructed a screw flight wear model verified by the experiment. The following conclusions were drawn.

- The proposed screw flight wear model was established based on Archard wear theory, which obtains the positive pressure of the scattered particles based on the continuous medium hypothesis method. The relationship between wear rate, rotational speed, and filling rate was obtained by numerical calculation.

- The accuracy of the relationship between the rotational speed and wear rate in the screw flight wear model was verified experimentally. The wear rate of the screw flight was approximately parabolic and increased with the increase in rotational speed. With the increase in rotational speed, the particle wear distance per unit time increased, which accelerated the surface wear of the screw flight.
- The influence of the filling rate in the screw flight wear model was studied and verified experimentally. The results showed that the screw flight wear rate was positively and linearly correlated with the filling rate. The increase in the filling rate led to an increase in the wear rate, which was caused by the increase in positive pressure F_n acting on the surface of the screw flight.

Acknowledgements

This study was financially supported by the National Natural Science Foundation Project of China under Grant 52075356, 2019 Key R&D project (International Scientific and Technological Cooperation) of Shanxi Province under Grant 201903D421005, Natural Science Foundation of Shanxi Province under Grant 201901D111246, Natural Science Foundation of Shanxi Province under Grant 201901D111236, and Graduate Education Innovation Project of Shanxi Province under Grant 2019BY119.

References

Archard, J.F. 1953. Contact and rubbing of flat surfaces. J. Appl. Phys. **24**(8): 981–988. doi:10.1063/1.1721448.

Bialobrzeska, B., and Kostencki, P. 2015. Abrasive wear characteristics of selected low-alloy boron steels as measured in both field experiments and laboratory tests. Wear, **328**: 149–159. doi:10.1016/j.wear.2015.02.003.

Chen, G., Schott, D.L., and Lodewijks, G. 2017. Sensitivity analysis of DEM prediction for sliding wear by single iron ore particle. Eng. Comput. **34**(6): 2031–2053. doi:10.1108/EC-07-2016-0265.

Forsström, D., and Jonsén, P. 2016. Calibration and validation of a large scale abrasive wear model by coupling DEM-FEM: Local failure prediction from abrasive wear of tipper bodies during unloading of granular material. Eng. Fail. Anal. **66**: 274–283. doi:10.1016/j.engfailanal.2016.04.007.

Gabler, H. 1981. Theoretische und experimentelle untersuchungen der forderung in steilen und senkrechten schneckenforderern. Thesis, Department of Mechanical Engineering, Technical University of Munich.

Gong, J., Fu, Y., Xia, W., Li, J., and Zhan, F. 2016. Fatigue life prediction of screw blade in screw sand washing machine under random load with gauss distribution. Am. J. Eng. Appl. Sci. **9**(4): 1198–1212. doi:10.3844/ajeassp.2016.1198.1212.

Janssen, H.A. 1895. Versuche Über Getreidedruck in Silozellen. Verein Dtsch. Ingenieur, **39**(35): 1045–1049.

Knuth, M.A., Johnson, J.B., Hopkins, M.A., Sullivan, R.J., and Moore, J.M. 2012. Discrete element modeling of a Mars exploration rover wheel in granular material. J. Terramech. **49**(1): 27–36. doi:10.1016/j.jterra.2011.09.003.

Moore, M.A. 1978. Abrasive wear. Int. J. Mater. Eng. Appl. **1**(2): 97–111. doi:10.1016/S0141-5530(78)90054-7.

Neuendorff, R. 1919. Die guldinschen rege. *In* Lehrbuch der Mathematik. *Edited by* R. Neuendorff Springer, Berlin, Heidelberg. pp. 200–204.

Piazzetta, G.R., Lagoeiro, L.E., Figueira, I.F.R., Rabelo, M.A.G., and Pintaude, G. 2018. Identification of abrasion regimes based on mechanisms of wear on the steel stylus used in the Cerchar abrasiveness test. Wear, **410**: 181–189. doi:10.1016/j.wear.2018.07.009.

Pratap, S., Nayak, A., Kumar, A., Cheikhrouhou, N., and Tiwari, M.K. 2017. An integrated decision support system for berth and ship unloader allocation in bulk material handling port. Comput. Ind. Eng. **106**: 386–399. doi:10.1016/j.cie.2016.12.009.

Rahmoun, J., Millet, O., and Saxcé, G.De. 2008. A continuous media approach to modeling the stress saturation effect in granular silos. J. Stat. Mech: Theory Exp. **2008**(06): P06011–P06019. doi:10.1088/1742-5468/2008/06/P06011.

Song, J., Feng, G., and Yuefeng, H. 1995. Lifting behavior of multi-thread screw ship unloader. J. Dalian Univ. Technol. **35**(2): 192–197.

Sun, X.X., Meng, W.J., and Yuan, Y. 2018. Conditions of gas–solid two-phase flow formed in a vertical screw conveyor. Adv. Mech. Eng. **10**(9): 1–10. doi:10.1177/1687814018797761.

Wang, R.Z., Mao, F.Z., Fang, X., Huang, Z., and Wang, B. 2019. Analysis of equivalent continuum model about activated coke particle in absorption tower. J. Heilongjiang Inst. Technol. Chinese, **19**(12): 84–89.

Wang, X., Li, B., and Yang, Z. 2018. Analysis of the bulk coal transport state of a scraper conveyor using the discrete element method. Stroj. Vestn. J. Mech. Eng. **64**(1): 37–46. doi:10.5545/sv-jme.2017.4790.

Wang, Y., Lu, Y., and Ooi, J.Y. 2015. A numerical study of wall pressure and granular flow in a flat-bottomed silo. Powder Technol. **282**: 43–54. doi:10.1016/j.powtec.2015.01.078.

Wang, Z., Wang, R., Fei, Q., Li, J., Tang, J., and Shi, B. 2017. Structure and microscopic wear analysis of lining material based on EDEM. MATEC Web Conf. **128**: 03001–03004. doi:10.1051/matecconf/201712803001.

Xia, R., Wang, X., Li, B., Wei, X., and Yang, Z. 2019. Discrete element method-(DEM-) based study on the wear mechanism and wear regularity in scraper conveyor chutes. Math. Probl. Eng. **2019**: 1–12. doi:10.1155/2019/4191570.

Yang, J. 2019. Study on abrasion of screw conveyor screw in sand mixing equipment. Petrol. Chemical Equip. Chinese, **4**(1): 5–9.